Discovery of isomers in dyprosium, holmium and erbium isotopes with N=94 to 97

T.P.D. Swan,[1,*] P.M. Walker,[1,2] Zs. Podolyák,[1] M.W. Reed,[1]
G.D. Dracoulis,[3] G.J. Lane,[3] T. Kibédi,[3] and M.L. Smith[3]

[1]*Department of Physics, University of Surrey, Guildford, Surrey GU2 7XH, United Kingdom*
[2]*CERN, CH-1211 Geneva 23, Switzerland*
[3]*Department of Nuclear Physics, RSPhysSE, Australian National University, Canberra ACT 0200, Australia*

(Dated: January 26, 2012)

High-spin states in the $^{164}_{68}Er_{96}$ region were studied using ^{9}Be + ^{160}Gd reactions. Pulsed beam conditions were exploited for enhanced sensitivity to delayed γ-ray transitions. New isomers were identified in ^{161}Dy, ^{163}Ho, ^{162}Er and ^{165}Er. The ^{162}Er isomer is interpreted to decay by E1 transitions to the ground-state-band (g.s.b.) with a reduced hindrance of f_ν=33. A plot of f_ν values for all ΔK=7, E1 transitions from two-quasiparticle isomers to the g.s.b. of even-even nuclei reveals only a small influence from the dynamic to kinematic moment-of-inertia ratio, which provides a measure of Coriolis K-mixing within the g.s.b. This is interpreted to imply that the relatively low hindrances are due to K-mixing in the isomer, caused by a combination of Coriolis and octupole band mixing.

PACS numbers: 23.35.+g, 21.10.-k, 21.10.Ky, 23.20.Lv

I. INTRODUCTION

The slow decay rates of isomers represent an extreme of nuclear conditions. The general features of this distinctive hindered decay behaviour are understood [1]. Despite these findings, interpreting the detailed differences between isomer decay rates remains a considerable challenge, and provides a tantalising opportunity to reveal less apparent features of nuclear structure.

An important degree of freedom is described by the K quantum number, the projection of angular momentum on the symmetry axis of the deformed nuclear shape. Decays from high-K states may be isomeric if available daughter levels represent a large change in K. Such decays should require a comparatively large multipole transition, λ. Nevertheless, low-multipole forbidden transitions are observed, which are hindered by the degree of forbiddenness, $\nu = \Delta K - \lambda$. In quantifying the hindrance of the decay, the half-life is measured relative to its Weisskopf estimate, $F_W = T^\gamma_{1/2}/T^W_{1/2}$. The influence of the forbiddenness on the hindered decay is described by the reduced hindrance, $f_\nu = F_W^{1/\nu}$ [2]. A wide range of f_ν values have been measured, demanding the consideration of other variables that affect decay rates, such as the reduction in K-conservation caused by mixing [3].

The Coriolis effect induces K-mixing by diverting the motion of nucleons in a rotating nuclear core. The effect reaches its greatest intensity for nucleons in high-j, low-Ω orbitals, where K=$\Sigma\Omega$ [4]. Similarly, the energy of an isomer relative to the yrast line can lead to small admixtures of low-K states through greater level density [5]. A third form of mixing arises through axial asymmetry in the nuclear shape, leading to a reduction in K-conservation [6]. Despite our understanding of K-mixing, additional experimental data are needed to reveal the more intricate mechanisms influencing the decay.

In order to observe these mechanisms, it is useful to plot f_ν values as a function of variables that quantify known mixing effects [2]. A recent publication [7] exploring the decay of an isomer in ^{162}Dy, showed the relation between f_ν and the product of the valence neutron and proton numbers, N_pN_n. For 2-quasiparticle isomers decaying by E2 transitions, N_pN_n, is well correlated with f_ν, but reveals a small additional influence from level density effects.

We now present new isomer data for other weakly populated nuclides in the same mass region. With focus on a K$^\pi$=7$^-$ isomer in ^{162}Er, f_ν is plotted as a function of the dynamic to kinematic moment-of-inertia ratio. This ratio gives a measure of Coriolis mixing in the daughter states of isomer decays to the ground-state band [8, 9].

II. EXPERIMENTAL DETAILS

In the present study, nuclei in the $^{164}_{68}Er_{96}$ region were populated using ^{9}Be + ^{160}Gd complete and incomplete fusion evaporation reactions. Pulsed and chopped beams were provided by the 14UD tandem accelerator at the ANU Heavy Ion Accelerator Facility [10] at an energy of 57 MeV. With the aim of measuring isomer properties in ^{164}Er [11], this beam energy provided the greatest cross section for ^{164}Er production through the ^{160}Gd(^{9}Be,5n) reaction. A highly enriched (> 95%) ^{160}Gd target with an effective thickness of 4.36 mg/cm^2 was placed at the centre of the Compton suppressed CAESAR array [12], consisting of 6 HPGe detectors at $\pm$48°, $\pm$97° and $\pm$147° in the beam plane, and 3 larger HPGe detectors, out of plane at $\pm$45° and +135°. The array includes 2 out of plane LEPS detectors at $-$90° and $-$135° for greater efficiency at low energies.

Chopped and bunched 1 ns beam pulses, with a 1.7 μs separation, were used to measure γ-ray events relative

*Electronic address: t.swan@surrey.ac.uk

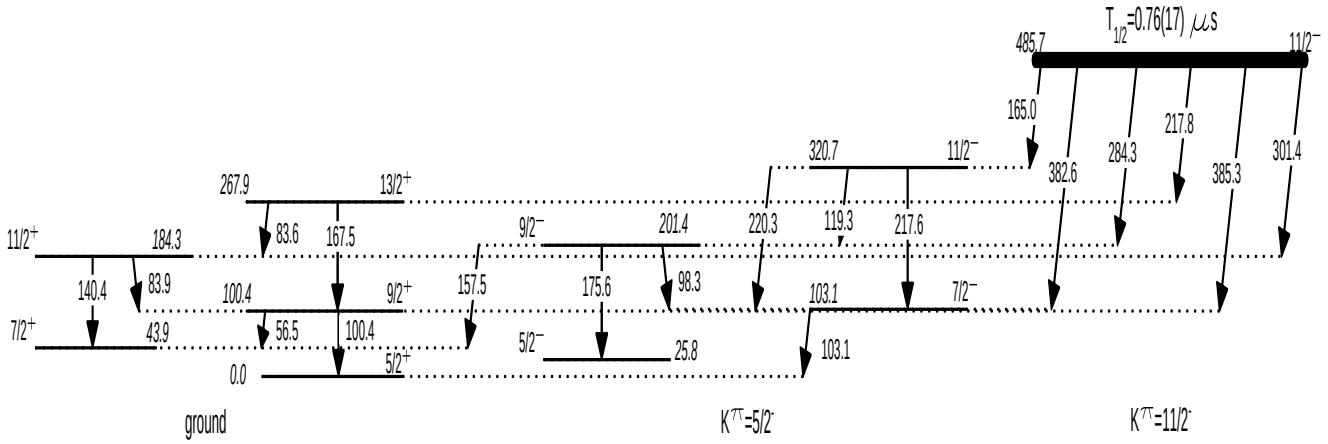

FIG. 1: Partial level scheme for $^{161}_{66}$Dy showing the newly identified isomer at 485.7 keV. All the transitions directly from the isomer are newly placed. Their relative intensities are given in Table I. Energies are in keV.

to the driving RF signal. These events were sorted into a "short time-γ" matrix (time vs energy). To measure life-times that were long compared to the 1.7 μs pulsing, another measurement was performed where the beam was chopped (30 μs on, 150 μs off) and γ-ray times were measured using a clock register relative to the driving RF to create a "long time-γ" matrix. Gamma-rays, detected between beam pulses, that were coincident within $\pm$150 ns were used to create an "out-of-beam γ-γ" matrix. Furthermore, in order to detect correlated events across isomeric states, an "early-delayed γ-γ" matrix was produced from events with a time difference of between 150 ns and 832 ns. The usual in-beam γ-γ coincidences were also studied.

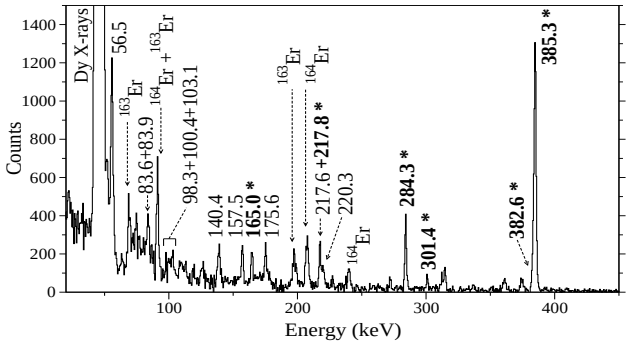

FIG. 2: Delayed coincidence spectrum for the early 156.1, 177.3, 198.2, 236.2, 375.5 and 415.7 keV transitions, showing decays from the $K^\pi=11/2^-$ isomer. Direct branches from the isomer are denoted by an asterisk. Random coincidences from ^{164}Er and ^{163}Er are labeled.

III. RESULTS

A. Isomer in ^{161}Dy

Recently, Jungclaus *et al.* [13] identified a rotational band above a $K^\pi=11/2^-$ band-head at 485.56 keV [14] in ^{161}Dy. The experiment had no out-of-beam condition, and no decays out of the band-head were observed. In the present work ^{161}Dy is populated through the (^{9}Be,α4n) channel. Coincidence measurements for γ-ray transitions between the low-spin members of the $K^\pi=5/2^-$ and $K^\pi=5/2^+$ bands (see figure 1) in the out-of-beam γ-γ matrix identified delayed γ-ray transitions from the 485.56 keV level, indicating an isomer. Despite a low efficiency due to a delayed coincidence width of 682 ns, the decay branches were more clearly resolved in the "early-delayed γ-γ" matrix by gating on a number of early transitions within the $K^\pi=11/2^-$ band [13], as seen in figure 2. Gamma coincidence measurements for the '217.6+217.8' peak confirmed it to be a doublet.

The relative intensities of the decay branches from the isomer are shown in table I. In agreement with Ref. [14], γ-ray energies place the isomeric state at 485.7(2) keV. Measurement of the half-life was hindered by the low yield, and by increased contamination from other delayed components at low energies. To measure the half-life, γ-ray energy spectra were produced from contiguous time regions in the short and long time-γ matrices, from which γ-ray intensity measurements were extracted for the 385.3 keV and 284.3 keV branches. The half-life of the ^{161}Dy isomer was determined (figure 3) to be 0.76(17) μs.

The $K^\pi=11/2^-$ isomer is known to have a 1-quasineutron, $\nu 11/2^-[505]$ orbital structure [14]. This structure is observed as an isomer in the nearby ^{163}Er and ^{165}Er nuclides, with half-lives of $T_{1/2} = 0.58$ μs [16] and $T_{1/2} = 0.25$ μs [17], and excitation energies of 445 keV and 551 keV, respectively. In figure 4 transition strengths for the decays from these isomers are compared, reflecting similarity in the decay paths and probabilities, and supporting the $\nu 11/2^-[505]$ assignment for the ^{161}Dy isomer.

B. Isomers in ^{163}Ho

A $K^\pi=17/2^+$ isomer has been observed previously in ^{163}Ho at a level energy of 1506 keV, decaying by a 973 keV transition to the ground-state band with a half-life

TABLE I: Gamma-ray energy, relative γ-ray branch intensity, transition strength, and reduced hindrance measurements for direct branches from the 485.6 keV, $K^\pi=11/2^-$ isomer in ^{161}Dy ($T^{exp}_{1/2}$ = 0.76*(17)* μs).

K^π_f	I^π_f	E_γ [keV]	I_γ	$\sigma\lambda$	α^a	Γ_γ [eV]	B($\sigma\lambda$) [W.u.]	ν	f_ν
$5/2^-$	$11/2^-$	165.0*(1)*	6.3*(6)*	[M1]	5.79×10^{-1}	2.5×10^{-8}*(6)*	2.6×10^{-7}*(7)*	2	1.94×10^{3}*(24)*
$5/2^+$	$13/2^+$	217.8*(1)*	4.1*(6)*	[E1]	3.89×10^{-2}	1.6×10^{-8}*(5)*	7.7×10^{-10}*(24)*	2	3.6×10^{4}*(5)*
$5/2^-$	$9/2^-$	284.3*(1)*	19*(1)*	[M1]	1.30×10^{-1}	7.5×10^{-8}*(18)*	1.6×10^{-7}*(4)*	2	2.5×10^{3}*(3)*
$5/2^+$	$11/2^+$	301.4*(1)*	3.4*(5)*	[E1]	1.70×10^{-2}	1.3×10^{-8}*(4)*	2.4×10^{-10}*(7)*	2	6.4×10^{4}*(9)*
$5/2^-$	$7/2^-$	382.6*(1)*	13*(2)*	[E2]	3.14×10^{-2}	5.1×10^{-8}*(14)*	1.5×10^{-4}*(4)*	1	6.7×10^{3}*(19)*
$5/2^+$	$9/2^+$	385.3*(1)*	100*(4)*	[E1]	9.36×10^{-3}	3.9×10^{-7}*(9)*	3.4×10^{-9}*(8)*	2	1.71×10^{4}*(20)*

[a] Electron conversion coefficients are obtained from Ref.[15].

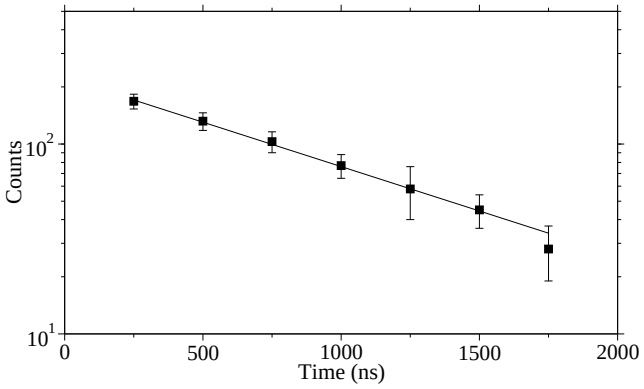

FIG. 3: One of the half-life plots for the delayed 385.3 keV transition, using 250 ns time regions in the long time-γ matrix. The half life for the ^{161}Dy isomer is 0.76(17) μs.

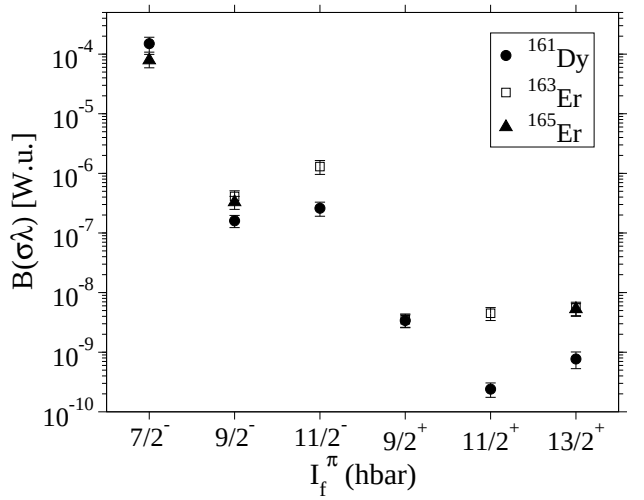

FIG. 4: Transition strengths for decay branches from the $K^\pi=11/2^-$ isomer in ^{161}Dy compared with the corresponding decays in ^{163}Er [16] and ^{165}Er [17]

of $T_{1/2} \geq 15$ ns [18] (see figure 5). The half-life measurement in the earlier work was limited by the loss of residual nuclei exiting the detection system. The same delayed transition was observed in the present work with an energy of 973.8 keV. A second much weaker branch from the same isomer was discovered at 581.1 keV (see figure 6(a)).

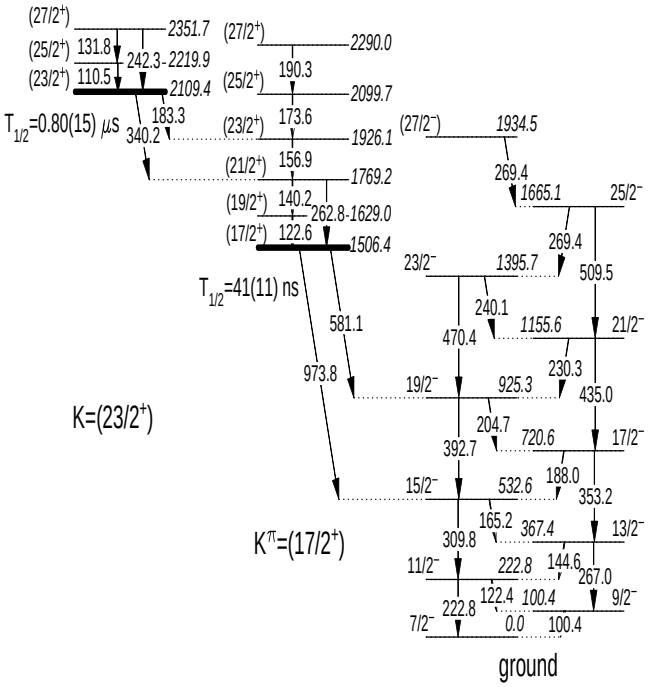

FIG. 5: Level scheme for $^{163}_{67}$Ho. The two half-lives are newly determined.

In the out-of-beam γ-γ matrix, a gate on the 973.8 keV transition yielded clear evidence for a second isomer, at 2109.4(2) keV, decaying by 340.2 and 183.3 keV γ-transitions into the known isomer band (see figure 6(b)). In figure 6(c), early coincidences with the delayed 340.2 and 973.8 keV transitions indicated three transitions within the 2109 keV isomer band.

The half-life of $T_{1/2}$= 0.80(15) μs for the 2109 keV isomer was obtained from a fit to the intensity of the 973.8 keV transition (figure 7), observed in γ-ray spectra produced from 156 ns wide time regions in the short time-γ matrix (direct branches from the isomer were heavily contaminated). Table II, shows that after 300 ns, all of the γ-ray intensity through the 1506 keV isomer comes from the 2109 keV isomer, and in figure 6(c), the band built on the 1506 keV isomer is not observed. This shows that the measured half-life is that of the 2109 keV isomer.

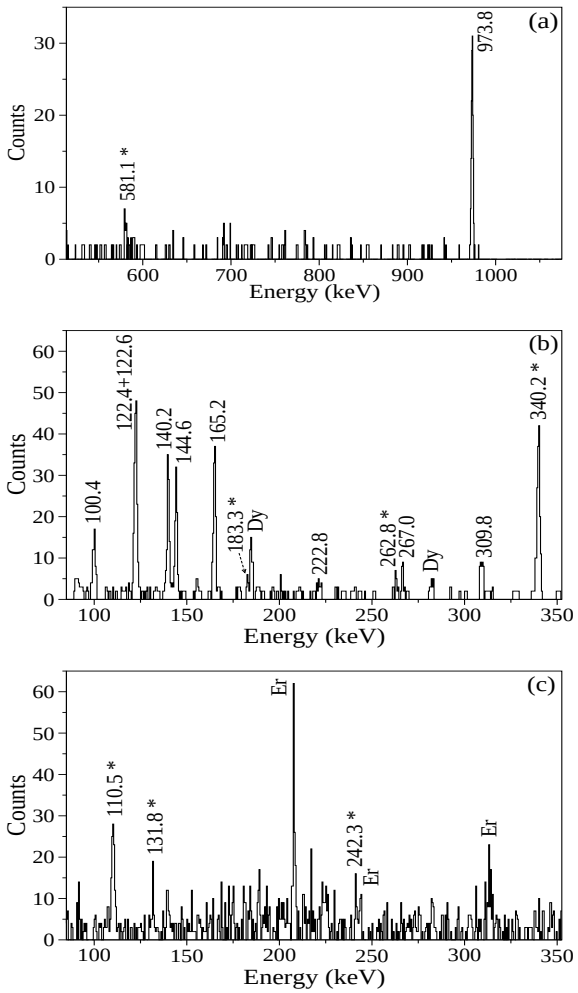

FIG. 6: (a) Coincidence spectrum for the 340.2 keV transition in the out-of-beam $\gamma-\gamma$ matrix in the 300-1550 ns range.(b) Coincidence spectrum for the 973.8 keV transition in the out-of-beam $\gamma-\gamma$ matrix in the 300-1550 ns range.(c) Early spectrum in coincidence with delayed 973.8 or 340.2 keV transitions. (all) New transitions are labelled with an asterisk, known ^{163}Ho transitions are labeled with their energy, and coincidences from ^{162}Dy and ^{164}Er are labeled Dy and Er.

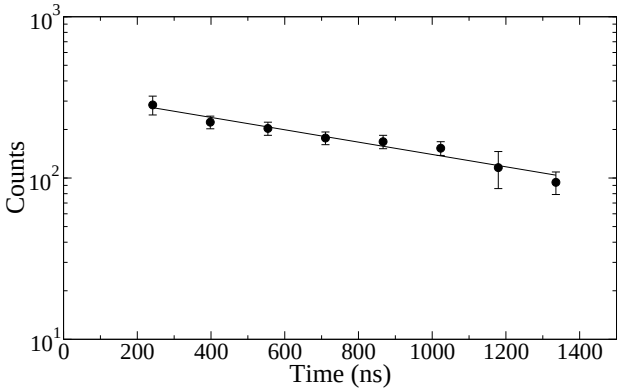

FIG. 7: Time spectrum for 973.8 keV γ-rays. The fitted half-life for the 2109 keV isomer is 0.80(15) μs.

Before 300 ns, a shorter delayed component was observed in the time spectrum for the 973.8 keV transition, with γ-ray coincidence spectra and intensity measurements showing this to be the 1506 keV isomer. The half-life of the 1506 keV isomer was measured in the short time-γ matrix with a background subtracted gate on 973.8 keV γ-rays. A measurement of $T_{1/2}$= 41(11) ns was obtained from the fit in figure 8. The fit is the sum of two exponentials, representing the two isomers, one of which is fixed at 0.80 μs.

TABLE II: Relative γ-ray intensities for transitions related to the isomers in ^{163}Ho. Top: Delayed transitions from the two isomers, as measured in the out-of-beam $\gamma-\gamma$ matrix in the 300-1550 ns range (intensity relative to 340.2 keV). Middle: Transitions above the new 2109 keV isomer (intensity relative to 110.5 keV). Bottom: Relative branch intensity for the newly discovered 262.8 keV transition.

E_γ(keV)	K_i^π	K_f^π	I_i^π	I_f^π	I_γ
340.2*(1)*	$(23/2^+)$	$(17/2^+)$	$(23/2^+)$	$(21/2^+)$	100 *(8)*
183.3*(1)*	$(23/2^+)$	$(17/2^+)$	$(23/2^+)$	$(23/2^+)$	6 *(2)*
581.1*(1)*	$(17/2^+)$	$7/2^-$	$(17/2^+)$	$19/2^-$	12 *(2)*
973.8*(1)*	$(17/2^+)$	$7/2^-$	$(17/2^+)$	$15/2^-$	89 *(8)*
110.5*(1)*	$(23/2^+)$	$(23/2^+)$	$(25/2^+)$	$(23/2^+)$	100 *(10)*
131.8*(1)*	$(23/2^+)$	$(23/2^+)$	$(27/2^+)$	$(25/2^+)$	28 *(6)*
242.3*(1)*	$(23/2^+)$	$(23/2^+)$	$(27/2^+)$	$(23/2^+)$	$\geq$26
140.2*(1)*	$(17/2^+)$	$(17/2^+)$	$(21/2^+)$	$(19/2^+)$	100 *(7)*
262.8*(1)*	$(17/2^+)$	$(17/2^+)$	$(21/2^+)$	$(17/2^+)$	20 *(4)*

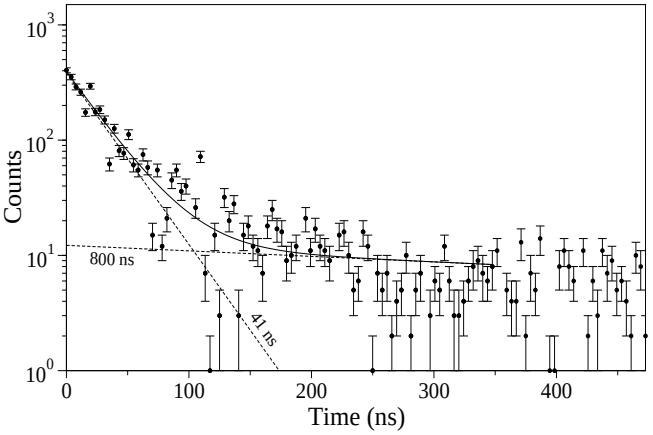

FIG. 8: Time spectrum for 973.8 keV γ-rays. The fitted half-life for the 1506 keV isomer is 41(11) ns. The solid line is a fit to the data including both isomer decays.

Considering the intensity of the branches (table II), the strength of the 973.8 keV transition relative to the 581.1 keV transition strongly favours a spin of 17/2 for the 1506 keV isomer, as a higher spin would require a higher multipole for the stronger transition, which is inconsistent with Weisskopf transition rate systematics [19, 20]. The weakness (or absence) of the 786 keV transition to the $17/2^-$ state at 721 keV is surprising, though a comparable situation is found for the E1 decay of a $19/2^-$ isomer in ^{153}Eu [21], and, to a lesser extent, for the $11/2^-$ isomer decay in ^{161}Dy (see section III A). For the 2109 keV isomer, the same systematics make a parent spin of 25/2

TABLE III: Gamma-ray energy, relative γ-ray branch intensity, transition strength, and reduced hindrance measurements for direct branches from the 2026.6 keV isomer in ^{162}Er ($T^{exp}_{1/2}$ = 88*(16)* ns), based on a K$^\pi$=7$^-$ assignment.

K^π_f	I^π_f	E_γ [keV]	I_γ	$\sigma\lambda$	α^a	Γ_γ [eV]	B($\sigma\lambda$) [W.u.]	ν	f$_\nu$
0^+	8^+	930.1*(4)*	31*(4)*	[E1]	1.57×10^{-3}	1.2×10^{-6}*(3)*	7.7×10^{-10}*(18)*	6	33.1*(13)*
0^+	6^+	1359.6*(2)*	100*(7)*	[E1]	8.90×10^{-4}	4.0×10^{-6}*(8)*	7.7×10^{-10}*(18)*	6	32.9*(12)*

[a] Electron conversion coefficients are obtained from Ref.[15].

unlikely, and the absence of a transition to the 19/2 level in the daughter band is consistent with such a transition having a higher multipole, favouring a spin of 23/2 for the isomer. Possible configuration assignments are discussed in section IV A.

C. Isomer in ^{162}Er

In the out-of-beam γ-γ matrix, a gate on the $6^+ \rightarrow 4^+$ (337.3 keV) ground-state band transition in ^{162}Er showed clear evidence for an isomer decaying by 1359.6 keV and 930.1 keV γ-transitions (see figure 9). The half-life of the isomer was measured in the short time-γ matrix with a background subtracted gate on 1359.6 keV γ-rays. A half-life of 88(16) ns was determined from the fit in figure 10.

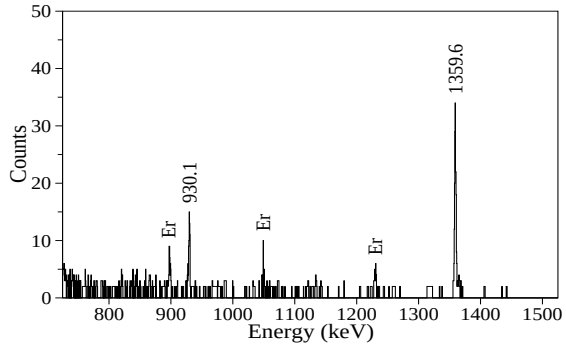

FIG. 9: Coincidence spectrum for the 337.3 keV transition in the out-of-beam $\gamma-\gamma$ matrix. Transitions in ^{162}Er are labeled with their energy. Random coincidences from ^{164}Er are labeled Er.

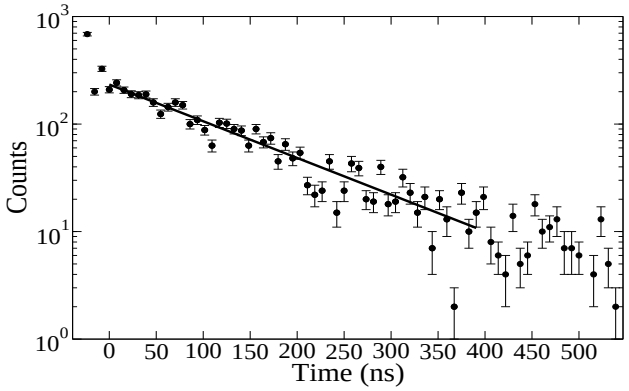

FIG. 10: Time spectrum for 1359.6 keV γ-rays. The fitted half-life is 88(16) ns.

The relative intensities, determined in the out-of-beam γ-γ matrix, are shown in table III. The γ-ray energies of these branches place the isomeric state at 2026.6(6) keV, in slight disagreement with a previous measurement of 2025.57(13) keV [22]. A partial level scheme is shown in figure 11. The two branches from the isomer have been previously reported by De Boer *et al.* [23] and Janssens *et al.* [22] with both works assigning a spin of 7 to the parent level on the basis of angular distributions. Neither work reported the level as an isomer. The level scheme is well established in these works.

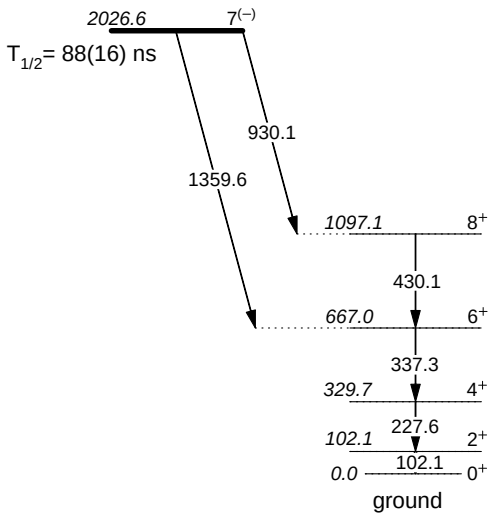

FIG. 11: Partial level scheme for ^{162}Er.

Regarding the spin-parity assignment of the isomer, its level energy and decay path are similar to that of a $K^\pi = 7^-$, 1985 keV isomer in ^{164}Er with a half-life of 23 ns [24]. Transition strengths for the direct branches from the two isomers are compared in figure 12. The ^{164}Er isomer principally decays to a K$^\pi$=5$^-$ band at the 6$^-$ and 7$^-$ levels, but equivalent branches are not observed for ^{162}Er. This likely stems from the K$^\pi$=5$^-$ band being further from yrast in ^{162}Er, as expected from single-particle excitation energies for the consituent $\nu 5/2^-[523]$ and $\nu 5/2^+[642]$ nucleons, which are higher in ^{161}Er compared with ^{163}Er and ^{165}Er [25]. The transition strengths to the $K^\pi = 0^+$ ground band are similar for both isomers. We therefore favour a $K^\pi = 7^-$ assignment for the ^{162}Er isomer. Its configuration and decay hindrance are discussed in section IV B.

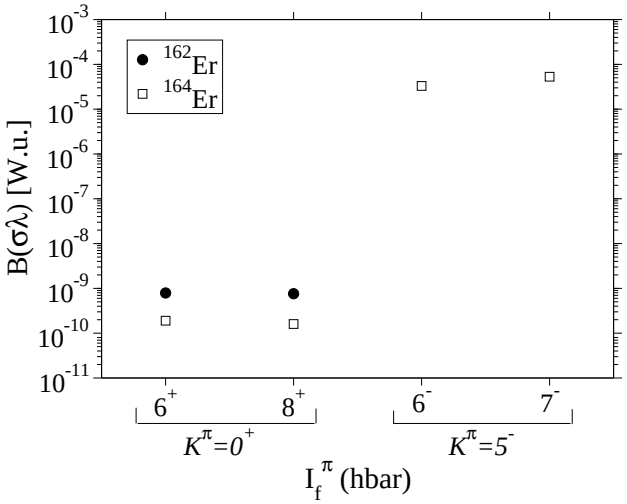

FIG. 12: Transition strengths for decay branches from the isomer in ^{162}Er compared with the decay of a $K^\pi = 7^-$ isomer in ^{164}Er [24] (the error bars are smaller than the data points).

D. Isomer in ^{165}Er

In the out-of-beam γ-γ matrix, a gate on the $13/2^- \rightarrow 11/2^-$ transition within the known K$^\pi$=11/2$^-$ isomer band in ^{165}Er (E=551 keV; $T_{1/2} = 0.25$ μs [17]) showed evidence for another isomer, at 1823.0(2) keV, decaying by a 317.0 keV γ-ray transition through an unknown band into the band based on the isomer (see figure 13(a)). Other direct branches from the new isomer at 1144.6 and 1050.6 keV (see figure 13(b)) were assigned. In figure 14 gates on the delayed 317.0, 799.8 and 623.6 keV transitions were summed within the "early-delayed γ-γ" matrix, isolating early transitions from two separate bands (bands "X" and "Y") that feed the isomer.

The half-life of the new isomer was measured within the short time-γ matrix with a background subtracted gate on the 799.8 keV transition (the intense 317.0 keV transition was contaminated with other delayed components). A measurement of $T_{1/2}$= 0.37(4) μs was determined from the fit in figure 15.

A partial level scheme is shown in figure 16. The measured γ-ray energies place the new isomer at 1823.0(2) keV. The 1823.0(2) keV level has been independently observed in a recent publication [26], in agreement with the excitation energy measured here, although it was not assigned as an isomer in that work. The 317.0, 799.8, 623.6, 767.2 and 188.2 keV transitions decaying from the 1823.0(2) keV level were also observed in that work.

The early transitions in figure 14 could not be detected in in-beam γ-γ coincidence measurements. However, ΔI=2 transitions allowed for some verification of ΔI=1 placements within bands X and Y. It is likely that one of the bands in early coincidence with decays from the isomer is its associated rotational band, with the other decaying into the isomeric state via an unobserved low energy transition.

Table IV contains relative intensities for the delayed transitions. The two branches from the isomer to known-

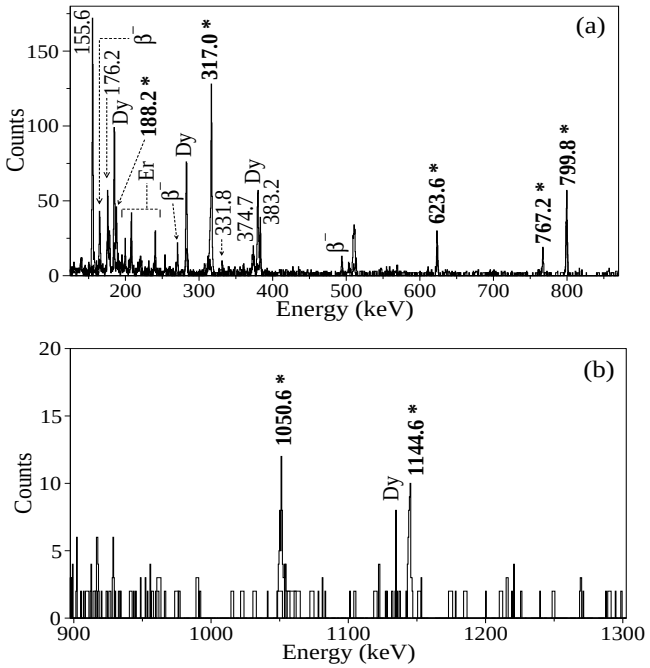

FIG. 13: Coincidence spectra in the out-of-beam $\gamma - \gamma$ matrix for transitions energies of: (a) 155.6 keV or 317.0 keV (b) 306.0, 259.6, 336.9, or 400.0 keV. New transitions following the decay of the 1823.0 keV isomer are denoted by an asterisk, known ^{165}Er transitions are labeled with their energy, and random coincidences from ^{164}Er, ^{162}Dy and ^{161}Tb are labeled Er, Dy and β^- respectively.

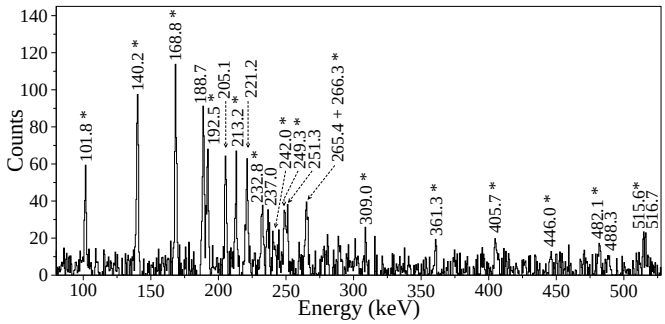

FIG. 14: Early spectrum in coincidence with delayed 317 keV, 800 keV or 624 keV γ-rays. Transitions within band X are denoted with an asterisk. Transitions within band Y are also labeled.

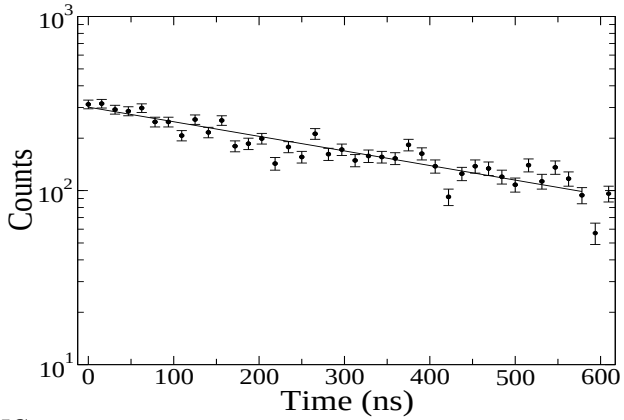

FIG. 15: Time spectrum for 799.8 keV γ-rays. The fitted half-life is 0.37(4) μs.

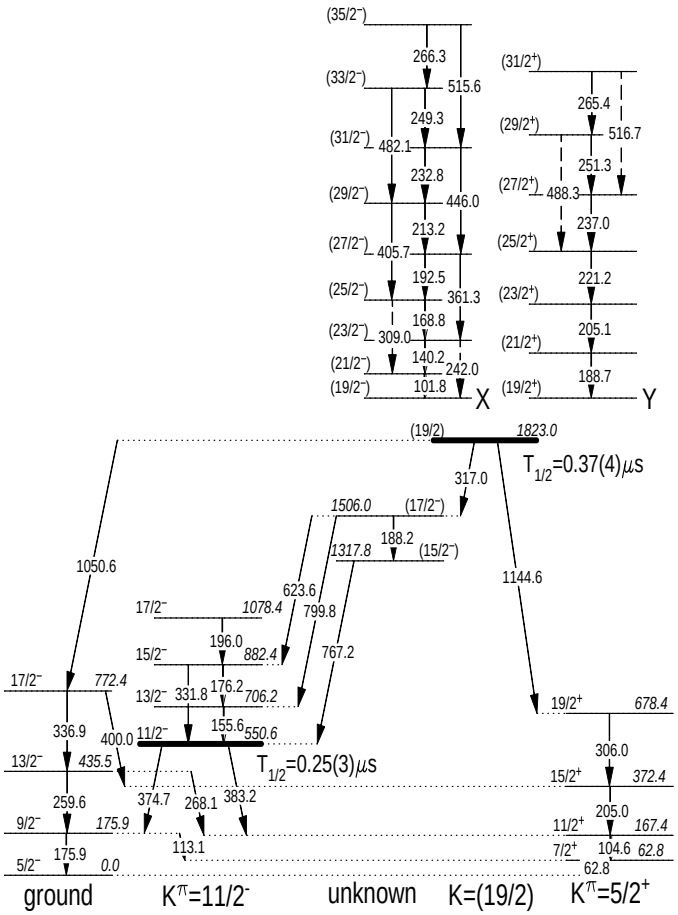

FIG. 16: Partial level scheme for ^{165}Er showing the decay of the new isomer ($T_{1/2}$= 0.37(4) μs). Spin and parity assignments for X and Y are tentative.

spin levels indicate an isomer spin of between 17/2 and 21/2 assuming dipole or quadrupole character. Table V contains relative intensities for transitions within bands X and Y. The tentative spin-parity assignments for bands X and Y (figure 16) are model dependent and are discussed in section IV C.

TABLE IV: Gamma-ray energy, relative γ-ray intensity, initial level energy, and final angular momentum for new delayed transitions in ^{165}Er. The uncertainty in the γ-ray energies is typically 0.1 keV

E_γ(keV)	I_γ	E_i	I_f^π
317.0	100 (8)	1823.0	$(17/2^-)$
1050.6	5 (1)	1823.0	$17/2^-$
1144.6	17 (2)	1823.0	$19/2^+$
188.2	13 (1)	1506.0	$(15/2^-)$
623.6	24 (2)	1506.0	$15/2^-$
799.8	62 (4)	1506.0	$13/2^-$
767.2	18 (2)	1317.8	$11/2^-$

TABLE V: Gamma-ray energy, relative intensity, initial level energy, initial angular momentum and final angular momentum for the two bands found to be feeding the new isomer in ^{165}Er. Top: band X (see figure 16). Bottom: band Y (see figure 16). Asterisks denote ΔI=2 transitions. The uncertainty in the γ-ray energies is typically 0.1 keV

E_γ(keV)	I_γ	E_i	I_i^π	I_f^π
101.8	40 (3)	1924.8	$(21/2^-)$	$(19/2^-)$
140.2	83 (8)	2065.0	$(23/2^-)$	$(21/2^-)$
168.8	100 (7)	2233.8	$(25/2^-)$	$(23/2^-)$
192.5	75 (6)	2426.3	$(27/2^-)$	$(25/2^-)$
213.2	61 (7)	2639.5	$(29/2^-)$	$(27/2^-)$
232.8	51 (5)	2872.3	$(31/2^-)$	$(29/2^-)$
249.3	45 (6)	3121.6	$(33/2^-)$	$(31/2^-)$
266.3	27 (6)	3387.9	$(35/2^-)$	$(33/2^-)$
(242.0)*	19 (7)	2065.0	$(23/2^-)$	$(19/2^-)$
(309.0)*	24 (8)	2233.8	$(25/2^-)$	$(21/2^-)$
361.3*	26 (4)	2426.3	$(27/2^-)$	$(23/2^-)$
405.7*	30 (10)	2639.5	$(29/2^-)$	$(25/2^-)$
446.0*	25 (3)	2872.3	$(31/2^-)$	$(27/2^-)$
482.1*	40 (7)	3121.6	$(33/2^-)$	$(29/2^-)$
515.6*	34 (6)	3387.9	$(35/2^-)$	$(31/2^-)$
188.7	95 (6)	2011.7	$(21/2^+)$	$(19/2^+)$
205.1	66 (6)	2216.8	$(23/2^+)$	$(21/2^+)$
221.2	70 (10)	2438.0	$(25/2^+)$	$(23/2^+)$
237.0	46 (7)	2675.0	$(27/2^+)$	$(25/2^+)$
251.3	40 (6)	2926.3	$(29/2^+)$	$(27/2^+)$
265.4	40 (6)	3191.7	$(31/2^+)$	$(29/2^+)$
(488.3)*	25 (6)	2926.3	$(29/2^+)$	$(25/2^+)$
(516.7)*	32 (6)	3191.7	$(31/2^+)$	$(27/2^+)$

IV. DISCUSSION

The isomers with unknown structure presented in section III were investigated with consideration of the intrinsic g-factor and alignment of the associated rotational bands, and through comparison with BCS calculations [27], which apply estimated pairing strengths to the Nilsson model to predict the energies of multi-quasiparticle states. A summary of these calculations is shown in table VI. Residual interactions are not included in the BCS calculations, but for 2-quasinucleon components the pairing energies (G_n, G_p) are adjusted to better reproduce configurations that are favoured by residual interactions. If included, the residual interaction would shift non-favoured configurations, such as the 7^+ state in table VI, up in energy by $\sim$ 200 keV [7].

A. ^{163}Ho

The structural assignments of the two isomers in ^{163}Ho, at 1506 keV and 2109 keV (see figure 5), were investigated. Transition intensities favour a spin of

TABLE VI: Predicted energies (E_{bcs}) for multi-quasiparticle states compared with experimentally determined energies (E_{exp}) for the isomers in section III.

Nucleus	E_{exp} (keV)	ϵ_2 [a]	ϵ_4 [a]	G_n/A (MeV)	G_p/A (MeV)	K^π(configuration)	E_{bcs} (keV)	Note[b]
^{163}Ho	1506	0.258	0.007	19.50	21.25	$17/2^+$ $(\pi 7/2^-[523]\nu 5/2^-[523]\nu 5/2^+[642])$	1504[c]	*(A)
						$17/2^-$ $(\pi 7/2^+[404]\nu 5/2^-[523]\nu 5/2^+[642])$	1944	*(B)
						$17/2^-$ $(\pi 7/2^-[523]\pi 7/2^+[404]\pi 3/2^+[411])$	1781	*(C)
^{163}Ho	2109	0.258	0.007	19.50	21.25	$23/2^-$ $(\pi 7/2^-[523]\nu 5/2^-[523]\nu 11/2^-[505])$	2314	*
						$23/2^+$ $(\pi 7/2^-[523]\nu 5/2^+[642]\nu 11/2^-[505])$	2334	*
						$25/2^+$ $(\pi 7/2^-[523]\nu 7/2^+[633]\nu 11/2^-[505])$	2598	
^{162}Er	2027	0.250	-0.007	20.23[d]	21.50[e]	7^- $(\pi 7/2^-[523]\pi 7/2^+[404])$	2023	*
						7^+ $(\nu 3/2^-[521]\nu 11/2^-[505])$	2333	
^{165}Er	1823	0.258	0.013	19.85[e]	21.50[e]	$19/2^+$ $(\nu 5/2^-[523]\pi 7/2^-[523]\pi 7/2^+[404])$	1893	*
						$19/2^-$ $(\nu 5/2^+[642]\pi 7/2^-[523]\pi 7/2^+[404])$	1940	*
						$21/2^-$ $(\nu 7/2^+[633]\pi 7/2^-[523]\pi 7/2^+[404])$	2359	
						$21/2^-$ $(\nu 11/2^-[505]\nu 5/2^-[523]\nu 5/2^-[512])$	2377	

[a] ϵ_2 and ϵ_4 values are from Ref.[28].
[b] Asterisk denotes configuration is discussed in the text.
[c] Fitted to the experimental energy by adjusting G_n and G_p.
[d] Fitted to the energy of a known 2-quasiparticle excitation.
[e] Estimated from neighboring nuclei.

$17/2$ for the 1506 keV isomer. Indeed, Hojman *et al.*[18] found reasonable evidence in favour of a $17/2^+$ $(\pi 7/2^-[523]\nu 5/2^-[523]\nu 5/2^+[642])$ configuration based on an observation of the same structure with a similar decay in ^{165}Tm [29]. BCS calculations predict three possibilities (see table VI) more yrast than any spin $19/2$ or $21/2$ configuration, these being the $17/2^+$ candidate configuration posited by Hojman, as well as $17/2^-$ $(\pi 7/2^+[404]\nu 5/2^-[523]\nu 5/2^+[642])$ and $17/2^-$ $(\pi 7/2^-[523]\pi 7/2^+[404]\pi 3/2^+[411])$, which will be referred to subsequently as A, B and C respectively.

The BCS calculations predict candidate A to be closest to yrast, 440 keV below the energy of B. As both A and B contain the 5^- $(\nu 5/2^-[523]\nu 5/2^+[642])$ 2-quasineutron component, the energy of the isomer may be compared with the energy of that configuration in neighbouring even-even nuclei. In ^{162}Dy this configuration is at an energy of 1486 keV, whilst for ^{164}Er it is at 1664 keV. These energies agree well with the 2-quasineutron component built upon the $\pi 7/2^-[523]$ ground-state band of ^{163}Ho, strongly favouring candidate A. Configuration B requires a much lower 2-quasineutron energy of $1506 - 440 = 1066$ keV, which is not favoured by these systematics.

Using rotational model formulae [30], intrinsic g-factors were extracted from the intensities in table II, giving $|g_K - g_R| = 0.22^{+0.04}_{-0.03}$, where Q_0=6.4 b is assumed from the β_2 deformation calculated in Ref.[28]. We compare the experimental value with the expected intrinsic g-factor for the three configurations. Using intrinsic spin g-factors of +5.59 and −3.83 for protons and neutrons respectively, with a quenching factor of 0.6, and assuming an effective $g_K = 0.08$ for $i_{13/2}$ neutrons [31], candidate A has $|g_K - g_R| = 0.41(5)$, B has $|g_K - g_R| = 0.13(5)$ and C has $|g_K - g_R| = 0.84(5)$. The value of the collective g-factor, g_R, can vary between configurations, and, in line with Refs.[31–33], we have used $g_R = 0.30(5)$. The g-factor evidence favours A and B more than C.

Additional information about band structure comes from the degree of rotation alignment, as described in Ref.[34]. In figure 17, the high alignment for the $17/2$ isomer band suggests the presence of the $5/2^+[642]$ neutron, further ruling out configuration C. Based on all these considerations, we tentatively favour candidate A, agreeing with the $17/2^+$ $(\pi 7/2^-[523]\nu 5/2^-[523]\nu 5/2^+[642])$ assignment of Hojman *et al.* [18].

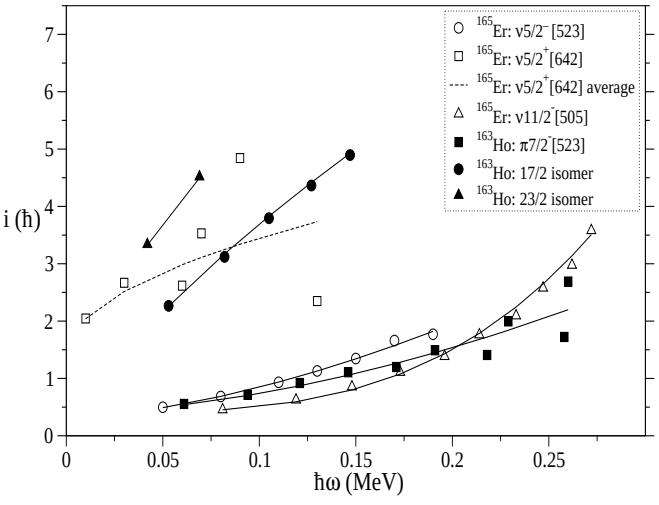

FIG. 17: Angular momentum alignment with the rotation axis for the bands identified in ^{163}Ho. One-quasineutron bands from ^{165}Er are compared. The Harris parameters are: $\mathcal{J}_0$=37 $\hbar^2 MeV^{-1}$; $\mathcal{J}_1$=42 $\hbar^4 MeV^{-3}$ [34].

Transition intensities for the newly discovered 2109 keV isomer indicate a band-head spin of 23/2. BCS calculations support this assignment, predicting a $23/2^-$ ($\pi 7/2^-[523]\nu 5/2^-[523]\nu 11/2^-[505]$) configuration at 2314 keV, and a $23/2^+$ ($\pi 7/2^-[523]\nu 5/2^+[642]\nu 11/2^-[505]$) configuration at 2334 keV. The intrinsic g-factors extracted from the intensities in table II give $|g_K - g_R| \leq 0.037$ compared to values of $|g_K - g_R| = 0.11(5)$ for the $23/2^-$ configuration, and $|g_K - g_R| = 0.02(5)$ for the $23/2^+$ configuration. This g-factor evidence favours the $23/2^+$ configuration.

The low energy $\Delta I = 1$ transitions for this band correspond to a high alignment (figure 17), suggesting the presence of the $5/2^+[642]$ neutron, and supporting the $23/2^+$ configuration. Thus, we tentatively assign a spin-parity of $23/2^+$ for the 2109 keV isomer.

B. ^{162}Er

For the ^{162}Er isomer presented in section III C, the spin 7 assignment for this level, reported by De Boer *et al.* [23] and Janssens *et al.* [22] on the basis of angular distributions, was supported by the similarity of the isomer's decay with that of a 7^- isomer in ^{164}Er. BCS calculations support this assignment further, predicting the 7^- ($\pi 7/2^-[523]\pi 7/2^+[404]$) only 4 keV from the experimental energy of the isomer (see table VI). In the absence of known 2-quasiproton structures in ^{162}Er, a proton pairing strength of G_p=21.5/A MeV was used as this predicts the energy of the 7^- configuration in ^{164}Er. Other I=7 configurations were predicted at least 300 keV above the experimental energy. No band was detected above the isomer, ruling out g-factor and alignment comparisons.

Both E1 transitions from the isomer have a reduced hindrance of f_ν=33 (see table III). This value may be compared with other 7^- isomers across the Segrè chart, revealing the effect of K-mixing on their decay rates. Figure 18 plots reduced hindrance as a function of the ground-state-band ratio of dynamic ($\mathcal{J}^1 = (2I-1)\hbar/E_\gamma(I)$) and kinematic ($\mathcal{J}^2 = 4\hbar^2/(E_\gamma(I+2) - E_\gamma(I))$) moments of inertia. This ratio gives a measure of rotational alignment in the ground-state-band, indicating the degree of K-mixing in the states fed by the isomer [8, 9].

All of the isomers in figure 18 possess a remarkably similar half-life (5 ns $\leq T_{1/2} \leq$ 100 ns), and this is reflected in their reduced hindrances, which are close to constant (the low value for ^{128}Ba is discussed later). In stark contrast, and building on Ref.[9], figure 19 is the comparative plot for 8^- isomers, showing a significant reduction in reduced hindrance as Coriolis K-mixing within the ground-state-band increases, before plateauing around the level of figure 18.

The lack of this relationship in figure 18 can be interpreted as due to K-mixing within the parent states of the ^{162}Er, ^{164}Er and ^{256}Fm isomer decays. In ^{256}Fm the $K^\pi=7^-$ isomer has a $\pi 7/2^+[633]\pi 7/2^-[514]$ configuration

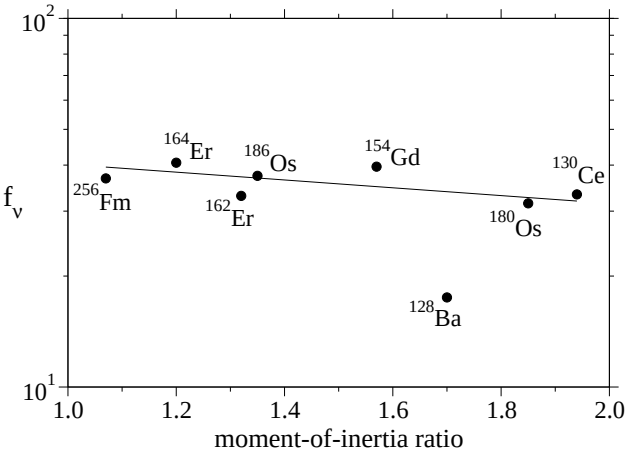

FIG. 18: Reduced hindrance values for ΔK=7, E1 transitions from two-quasiparticle isomers in even-even nuclei [24, 35–40]. The horizontal axis is the ratio of the ground-state-band dynamic and kinematic moments of inertia. The line is to guide the eye.

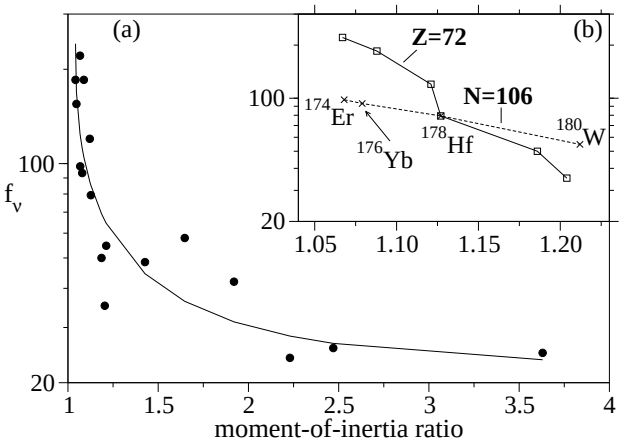

FIG. 19: (a) Reduced hindrance values for ΔK=8, E1 transitions from two-quasiparticle isomers in even-even nuclei [9, 41, 42]. The horizontal axis is the ratio of the ground-state-band dynamic and kinematic moments of inertia. The line is to guide the eye. (b) Showing [9] only the Z=72 and N=106 isomers from (a).

[40] resulting in a large Coriolis mixing matrix element from the presence of an $i_{13/2}$ proton. This can lead to a low reduced hindrance as seen in figure 19(b), which compares Z=72 and N=106, $K^\pi=8^-$ isomers. As discussed in Ref.[41], for N=106 the $\nu 7/2^-[514]\nu 9/2^+[624]$ configuration of the ^{174}Er and ^{176}Yb, $K^\pi=8^-$ isomers, which involves an $i_{13/2}$ neutron, results in relatively low f_ν values. Indeed, in ^{178}Hf (Z=72), mixing of this 2ν state with the $\pi 7/2^+[404]\pi 9/2^-[514]$ configuration, which is assigned to all of the isomers in Z=72 nuclei, has resulted in a low f_ν value [43]. The ^{162}Er and ^{164}Er, $K^\pi=7^-$ isomers in figure 18 have $\pi 7/2^+[404]\pi 7/2^-[523]$ configurations, which like the Z=72, $K^\pi=8^-$ isomers in figure 19 do not include an $i_{13/2}$ nucleon. However, the lower Ω value of the $h_{11/2}$ orbital in the $K^\pi=7^-$ isomers could contribute to greater Coriolis mixing and a lower reduced hindrance.

Alternatively, the large discrepancy between $K^\pi=7^-$ and $K^\pi=8^-$ isomers at low moment-of-inertia ratios may be attributable to mixing of a $K^\pi=0^-$ octupole band with the $K^\pi=7^-$ isomers [44]. The low-K admixture of this band will not be seen in $K^\pi=8^-$ isomers due to the symmetry properties of $K^\pi=0^-$ octupole bands, which forbid even-spin states. Octupole mixing with a rotational band built on an isomer has been observed, for example, in ^{170}Yb [45], where a significant reduction in the hindrance of transitions to the ground-state band from the odd-spin states was observed, compared to the transitions from the even-spin states. For $K^\pi=7^-$ isomers, mixing of this variety could reduce the dependence of the reduced hindrance on ground-state-band Coriolis K-mixing.

A more quantitative approach to the description of the $K^\pi=8^-$ isomers was taken by Dracoulis *et al.*[41] by evaluating the Coriolis K-mixing in the isomer configuration. It would be useful to extend that approach to the $K^\pi=7^-$ isomers.

There is one outlier in figure 18, the ^{128}Ba isomer, which can be explained in terms of additional K-mixing within the isomer state due to a chance near-degeneracy. A 7^- level which decays via a $T_{1/2}$=3.6 ps, E1 transition to the ground-state-band is observed 17 keV above the energy of the 6.1 ns isomer [35]. A two-band mixing analysis reveals that a mixing matrix element of 0.43 keV leads to a 0.06% admixture of the fast decaying state into the isomer, sufficient to explain the low hindrance of its decay [3].

C. ^{165}Er

The daughter level spins following two transitions from the newly discovered isomer in ^{165}Er (see figure 16), indicated a parent level spin of between 17/2 and 21/2. BCS calculations predict a $19/2^+$ ($\nu5/2^-[523]\pi7/2^-[523]\pi7/2^+[404]$) configuration 70 keV above the experimental energy of 1823 keV, and a $19/2^-$ ($\nu5/2^+[642]\pi7/2^-[523]\pi7/2^+[404]$) configuration 117 keV above the experimental energy (see table VI). The likelihood of these two configurations being the bands labeled X and Y in figure 16 is enhanced by the remarkable similarity with the level structure observed in ^{163}Er [46].

Intrinsic g-factors were extracted for band X, which has confirmed ΔI=2 transitions (see top half of table V for intensities). These are summarised in table VII and indicate $|g_K - g_R| = 0.33(2)$. Using the values detailed in section IV A, the theoretical g-factor for the $19/2^+$ configuration was calculated to be $|g_K - g_R| = 0.56(5)$, and for the $19/2^-$ configuration $|g_K - g_R| = 0.46(5)$. The g-factors marginally favour the $19/2^-$ configuration for band X.

As the $19/2^-$ and $19/2^+$ configurations both contain the 7^- ($\pi7/2^-[523]\pi7/2^+[404]$) 2-quasiproton excitation coupled with either the $\nu5/2^+[642]$ or $\nu5/2^-[523]$ neutron, there should be a considerable difference in the alignment of the two configurations, reflected by the difference in alignment for the 1-quasineutron $\nu5/2^+[642]$ and $\nu5/2^-[523]$ bands in ^{165}Er. Figure 20 plots the alignment of these structures, confirming that band X is more aligned than band Y by a difference approximately equal to the difference in aligment of the $\nu5/2^+[642]$ and $\nu5/2^-[523]$ bands. This is strong evidence that band X contains the $\nu5/2^+[642]$ neutron from the $19/2^-$ configuration, agreeing with the g-factor measurement. We therefore favour a band-head spin-parity of $19/2^-$ for band X, and $19/2^+$ for Y.

It is not possible to assign the $19/2^+$ or $19/2^-$ bands to the isomer. We can only state that both bands decay through the isomer, as both are in early coincidence with respect to the delayed isomeric transitions. It is highly likely that one of these bands is the isomer band, while the other decays into the isomer band-head through a low energy E1 transition (<60 keV). This transition may be obscured by strong X-rays between 40 and 60 keV.

TABLE VII: Intrinsic g-factors for the newly identified band X in ^{165}Er. Calculations assume $K = 19/2$, and a quadrupole moment of $Q_0 = 6.6$ b [28].

I_i, K	$\lvert g_K - g_R\rvert$
27/2,19/2	0.31^{+5}_{-3}
29/2,19/2	0.33^{+10}_{-7}
31/2,19/2	0.39^{+5}_{-4}
33/2,19/2	0.33^{+6}_{-5}
35/2,19/2	0.31^{+7}_{-7}

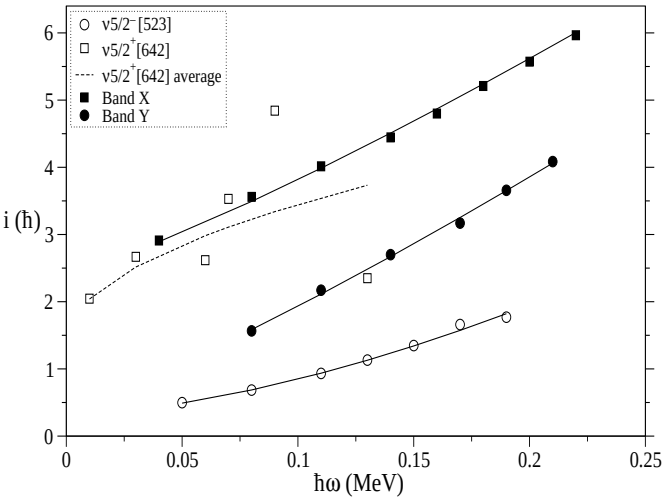

FIG. 20: Net angular momentum alignment for the two new bands, the $\nu5/2^+[642]$ band, and the $\nu5/2^-[523]$ band in ^{165}Er. The Harris parameters are: $\mathcal{J}_0$=37 $\hbar^2 MeV^{-1}$; $\mathcal{J}_1$=42 $\hbar^4 MeV^{-3}$ [34].

V. SUMMARY

Four isomers have been discovered in N=94-97 dysprosium, holmium and erbium isotopes. Half-life measurements were obtained and structural assignments were proposed on the basis of decay branch transition rates, multi-quasiparticle calculations, and the intrinsic g-factor and alignment of their associated rotational bands.

An isomer in ^{162}Er, which decays by E1 transitions to the ground-state band with a reduced hindrance of f_ν=33, is compared with other $K^\pi=7^-$ isomers with similar decay characteristics on a plot of f_ν versus the dynamic to kinematic moment-of-inertia ratio. The near constant f_ν values over the full moment-of-inertia ratio range, a feature not seen for $K^\pi=8^-$ isomers, suggests the dominant K-mixing in these isomers occurs in the isomer itself rather than the daughter state. This mixing is interpreted as being caused by a combination of Coriolis effects due to the occupation of high-j, lower-Ω orbitals in $K^\pi=7^-$ isomers, and band mixing from the $K^\pi=0^-$ octupole band.

This work has been supported by the UK STFC, and AWE plc.

[1] P. M. Walker & G. D. Dracoulis, Nature **399**, 35 (1999).
[2] P. M. Walker & G. D. Dracoulis, Hyp. Int. **135**, 83 (2001).
[3] G. D. Dracoulis *et al.*, Phys. Rev. Lett. **97**, 122501 (2006).
[4] F. S. Stephens, Rev. of Mod. Phys. **47**, 1 (1975).
[5] P. M. Walker *et al.*, Phys. Lett. B **408**, 42 (1997).
[6] G. J. Lane *et al.*, Phys. Rev. C **82**, 051304(R) (2010).
[7] T. P. D. Swan *et al.*, Phys. Rev. C **83**, 034322 (2011).
[8] P. M. Walker *et al.*, Phys. Rev. C **49**, 1718 (1994).
[9] P. M. Walker, Nucl. Phys. A **834**, 22c (2010).
[10] G. D. Dracoulis, Nucl. Phys. News **9**, 1 (1999).
[11] T. P. D. Swan *et al.*, to be published.
[12] G. D. Dracoulis and A. P. Byrne, ANU-P/1052(1995)115 (1995) unpublished.
[13] A. Jungclaus *et al.*, Phys. Rev. C **67**, 034302 (2003).
[14] V. A. Bondarenko *et al.*, Proc. 33rd Annual Conference on Nuclear Spectroscopic Structures in Atomic Nuclei (1983) Moscow.
[15] T. Kibédi *et al.*, Nucl. Instr. and Meth. A **589**, 202-229 (2008).
[16] P. O. Tjom and B. Elbek, Mat. Fys. Medd. Dan. Vid. Selsk **37**, 7 (1969).
[17] W. Andrejtscheff *et al.*, Nucl. Phys. A **220**, 438 (1974).
[18] D. Hojman *et al.*, Eur. Phys. Jour. A **21**, 383 (2004).
[19] K. E. G. Lobner, Phys. Lett. B **26**, 369 (1968).
[20] R. B. Firestone and V. S. Shirley (eds), Table of Isotopes, 8th Edition, Wiley, 1996.
[21] J. F. Smith *et al.*, Phys. Rev. C **62** 034312 (2000).
[22] R. Janssens *et al.*, Nucl. Phys. A **283**, 493 (1977).
[23] F. W. N. De Boer *et al.*, Nucl. Phys. A **236**, 349 (1974).
[24] F. W. N. De Boer *et al.*, Nucl. Phys. A **169**, 577 (1971).
[25] A. K. Jain *et al.*, Rev. Mod. Phys. **62**, 2 (1990).
[26] S. Wang *et al.*, Phys. Rev. C. **84**, 037303 (2011).
[27] K. Jain *et al.*, Nucl. Phys. A **591**, 61 (1995).
[28] P. Moller *et al.*, Atom. Dat. & Nucl. Dat. Tab. **59**, 185 (1995).
[29] H. J. Jensen *et al.*, Nucl. Phys. A **695**, 3 (2001).
[30] A. Bohr and B. R. Mottelson, Nuclear Structure vol. 2 (1975) New York: Benjamin.
[31] P. M. Walker *et al.*, Nucl. Phys. A **568**, 397 (1994).
[32] T. P. D. Swan, Ph.D. Thesis, University of Surrey (2011).
[33] S. M. Mullins *et al.*, Phys. Lett. B **393**, 279 (1997).
[34] S. Frauendorf, Phys. Scripta, **24**, 349 (1981).
[35] O. Vogel *et al.*, Eur. Phys. J. A **4**, 323 (1999).
[36] D. M. Todd *et al.*, J. Phys. G: Nucl. Phys. **10**, 1407 (1984).
[37] J. F. Sharpey-Schafer *et al.*, Eur. Phys. J. A **47**, 5 (2011).
[38] R. M. Lieder *et al.*, Nucl. Phys. A **645**, 465 (1999).
[39] C. Wheldon *et al.*, Nucl. Phys. A **652**, 103 (1999).
[40] F. R. Xu *et al.*, Phys. Rev. Lett. **92**, 252501 (2004).
[41] G. D. Dracoulis et al., Phys Rev C **79**, 061303(R) (2009).
[42] International Network of Nuclear Structure and Decay Data Evaluators, Evaluated Nuclear Structure and Decay data File (ENSDF), http://www-nds.iaea.org/nsdd.
[43] T. L. Khoo *et al.*, Phys. Lett. B **67**, 3 (1977).
[44] P. M. Walker, Hyp. Int. **143** 143 (2002).
[45] P. M. Walker *et al.*, Phys. Lett. B**86**, 1 (1979).
[46] G. B. Hagemann *et al.*, Nucl. Phys. A **618**, 199 (1997).